



Retention and release of deuterium implanted in copper coatings on Al-6061

M.Y. Inal^a, M. Alam^{a,*}, K. Kurz^b, D.F. Cowgill^b, R.A. Causey^b

^a *Department of Materials and Metallurgical Engineering, New Mexico Institute of Mining and Technology, 801 Leroy Place, Socorro, NM 87801-4796, USA*

^b *Sandia National Laboratories, Livermore, CA 94550, USA*

Received 16 August 1999; accepted 20 October 1999

Abstract

To mitigate the problem of retention and permeation of tritium implanted in Al-6061, the use of copper coatings was investigated. Copper coatings (having weights of 0.03, 0.06 and 0.088 kg/m²) deposited on Al-6061 substrates by the RF Magnetron sputtering method were implanted with deuterium (D) in an accelerator at 350 K, and the resulting D profiles were monitored using negative SIMS and the D(³He,p)⁴He nuclear reaction. The retention characteristics of deuterium were subsequently studied as a function of coating weight, D⁺ fluence (varied in the 1–3 × 10²¹ D⁺/m² range) and D⁺ ion energy (40 and 120 keV). Under identical implantation conditions, deuterium retention in Al-6061 was higher than in Al-6061 coated with 0.088 kg/m² Cu. In the various coatings implanted under different conditions, deuterium retention ranged between 1.2% and 5.4% of the implanted amount. The deuterium retention decreased with increasing coating weight and then leveled off with further increases in the coating weight. The retention increased linearly with implantation fluence. © 2000 Published by Elsevier Science B.V. All rights reserved.

1. Introduction

Tritium has traditionally been produced by the ⁶Li(n,⁴He)³H nuclear reaction [1]. The source of neutrons has been the nuclear fission reactions occurring inside of nuclear reactors. Nuclear fission is not an environmentally friendly process because of the generation of long-lived radioactive products such as plutonium and neptunium [2]. Neutrons, however, may be produced by other mechanisms such as spallation [3]. Recently there has been an attempt to explore the usage of spallation neutrons for the production of tritium via the ³He(n,p)³H nuclear reaction [4]. In this process, protons are accelerated to very high energies in a linear accelerator and slammed into a heavy metal target. The resulting spallation neutrons are slowed down in water before interacting with ³He gas contained inside Al-6061 tubes (selected because of their

low neutron capture cross-section). This process, referred to as the Accelerator Production of Tritium (APT) process, has many advantages over tritium production in nuclear reactors, such as no radioactive waste generation, no chance of a criticality accident, possibility of immediate shutdown and no nuclear proliferation concerns [2]. The major disadvantage is obviously the high cost.

Some of the APT design features have recently been discussed [5]. The ³He(n,p)³H nuclear reaction occurring inside the Al-6061 tubes produces tritium with a kinetic energy of ~192 keV. Due to the high energy, a sizable fraction of tritium (~15%) is predicted to be implanted into the tube walls. The implanted tritium atoms will respond in three ways: (a) diffuse to the inside surface, recombine on this surface and enter into the ³He gas stream by desorption (release process); (b) diffuse to the outside surface, recombine on that surface and enter into the surrounding cooling water (permeation process); and (c) remain trapped in the walls at defect sites (retention process). The last two scenarios are not

* Corresponding author.

desirable, and there is a need to minimize both the permeation and the retention of the implanted tritium. This can be accomplished by maximizing the rate of release of tritium from the inside surface. The overall release process involves three consecutive steps: transport from the implant region to the inside surface, surface recombination and desorption. Desorption of molecular hydrogen from metal surfaces is a relatively fast process and is not considered to be the rate limiting step [6]. Therefore, either the transport step, or the recombination step, or both may limit the release rate. Transport of hydrogen isotopes in aluminum and their recombination on aluminum surfaces have been studied extensively. It has been observed that the diffusing hydrogen isotopes are trapped at implantation induced defect sites [7–10]. Furthermore, the presence of surface oxygen, particularly in the form of an oxide, severely degrades the recombination kinetics [11–13]. Both these effects lead to slower release kinetics and correspondingly higher permeation rate and retention.

The tritium permeation and retention problem can be mitigated by the use of coatings on the inside surface of ^3He containing tubes. The coating materials should have high diffusivity for tritium and should be weak oxide formers, to allow for rapid migration of tritium and subsequent atomic recombination on the surface. The coating thickness should be such that tritium is implanted in the coating and not the underlying tube wall. A potential candidate in this regard is copper. Although, the diffusivities of hydrogen isotopes in un-irradiated Al and Cu are roughly similar [14], implantation induces more defects in Al as compared to Cu because of the higher number of atomic displacements induced in Al as compared to Cu per implanted hydrogen ion [15]. Therefore, the effective hydrogen isotope diffusivity is likely to be higher in irradiated Cu as compared to irradiated Al. Furthermore, Cu is a weaker oxide former than Al [16]. Both these factors should cause the implanted tritium to be released at a higher rate from Cu as compared to Al, resulting in lower permeation and retention of tritium. The objective of this paper is to report experimental data on tritium inventory in the ^3He containing Al-6061 tube material coated with copper. The data are obtained by accelerator implantation of deuterium in flat copper-coated Al-6061 coupons as a function of copper coating thickness, deuterium ion fluence and deuterium ion energy. Deuterium is used to simulate the effects of tritium because of the high radioactivity of tritium.

2. Experimental

Copper coatings were prepared on $17 \times 17 \times 0.82 \text{ mm}^3$ size substrates of Al-6061 by the RF Magne-

tron sputter deposition method. The details of the deposition system and the deposition procedure are given elsewhere [5]. Magnetron sputtering is used in this study only to demonstrate the concept. It is understood that this method of deposition is not viable for coating the interiors of long and narrow tubes. Discs of 8 mm diameter were punched out from the square samples for deuterium implantation. The details of the accelerator and the implantation procedure are given elsewhere [17]. During implantation, sample temperature, chamber pressure and deuterium ion flux were held constant at $350 \pm 4 \text{ K}$, $\leq 6 \times 10^{-4} \text{ Pa}$, and $1.1 \times 10^{17} \text{ D}^+/\text{m}^2 \text{ s}$, respectively. Coatings of three different thicknesses corresponding to coating weights of 0.030, 0.060 and 0.088 kg/m^2 were used. The bare aluminum samples and the copper coated samples studied under the different implantation conditions are listed in Table 1. The ion energies studied were either monoenergetic (40 keV) or multienergetic (40 and 120 keV), and in the case of multienergetic implants equal fluences were used at the two ion energies.

Deuterium depth profiles were measured using the Cameca ims 5f secondary ion mass spectrometer (SIMS). Sputtering was accomplished by a Cs^+ primary ion beam under the following conditions: primary beam voltage = 10 kV, sample bias = -4.5 kV, primary beam current = 30 nA, primary beam incidence angle = 24.5° (relative to surface normal of the sample), penetration depth = 10.3 nm and beam diameter = 50 μm . The chamber was outgassed to about $9.3 \times 10^{-8} \text{ Pa}$ before starting the analysis. The primary ion beam was rastered over an area of $200 \times 200 \mu\text{m}^2$, while the negative secondary ions were analyzed from only the central 30 μm in order to eliminate spurious ions from the crater edges. Sputtering rates were determined by measurements of the sputtered crater depths using the Dektak³ST surface profilometer with a 2.5 μm diameter stylus, and dividing the measured crater depths with the total sputtering times. There was a lag time between deuterium implantation and SIMS measurements. First SIMS measurement was performed five days after deuterium implantation and it took three days to conduct all the SIMS measurements. During this lag time, samples were stored at room temperature.

SIMS analysis provided qualitative data. The qualitative SIMS data were quantified by performing nuclear reaction analysis (NRA) on selected samples. A ^3He beam at 650 keV was used to profile deuterium by detecting the proton yield due to the $\text{D}(^3\text{He},\text{p})^4\text{He}$ nuclear reaction. The beam current over an area of $2 \times 10^{-6} \text{ m}^2$ was 30 nA and the total fluence was $5 \times 10^{17} \text{ }^3\text{He}/\text{m}^2$. The deuterium counts were calibrated against an ErD_2 standard sample. Due to limited resolution of the profiling technique, the data were obtained up to a depth of 0.5 μm below the surface.

Table 1
Samples implanted with deuterium and the implantation conditions

Sample identification	Coating weight (kg/m ²)	Deuterium fluence 10 ²¹ (D ⁺ /m ²)	Ion energy (keV)
1	0.000	1	40
2	0.000	1	40 + 120
3	0.030	1	40
4	0.060	1	40
5	0.088	1	40
6	0.060	2	40
7	0.060	3	40
8	0.030	1	40 + 120
9	0.060	1	40 + 120
10	0.088	1	40 + 120
11	0.060	2	40 + 120
12	0.060	3	40 + 120

3. Results and discussion

3.1. Coating characteristics

Copper coatings having weights of 0.03, 0.06 and 0.088 kg/m² were studied. Assuming the coatings to be uniform, dense and single phase Cu, the corresponding thicknesses were calculated to be 3.3, 6.7 and 9.8 μm, respectively. The coatings had 0.5–2 μm size grains and had a surface roughness of ±250 nm over a 2.5 μm distance. All the coatings contained intermetallic phases Cu₉Al₄ and CuAl₂ beside Cu. The fraction of Al in any coating increased with increasing depth below the surface. Furthermore, the fraction of Al on the coating surface decreased with increasing coating weight. Pole figure measurements indicated fiber texture in the coatings. Both Cu and CuAl₂ phases in the coatings were in a state of compression. In the 0.06 kg/m² coating, isotropic plane stresses in Cu and CuAl₂ were –25 and –189 MPa, respectively. The coating-substrate bond strength (as measured by the tensile pull testing) was better than 2 MPa. Deuterium implantation did not affect the microstructure (as observed by SEM and AFM), texture and the bond strength. However, the residual compressive stresses in both phases initially decreased with increasing ion energy and fluence, and then increased again with further increases in ion energy and fluence. The details can be found in Refs. [5,17].

3.2. Deuterium depth calculations

To assess the depth of implantation of deuterium in the coatings at the two different ion energies (40 and 120 keV), a computer simulation program, TRIM was used [18]. Since all the coatings contained Cu₉Al₄ and CuAl₂ phases beside Cu, deuterium implantation depth profiles were calculated in each phase along with that in Al for comparison purposes. The input data on mass, density,

displacement energy and lattice binding energy for the simulation were taken from published literature [18–20]. The calculated depth profiles are shown in Fig. 1. The deuterium implantation depth is higher and the deuterium profile is narrower in Al as compared to Cu. The two intermetallic phases reveal a behavior which is intermediate between that of Al and Cu, with higher implantation depth in the Al-rich CuAl₂ as compared to the Cu-rich Cu₉Al₄.

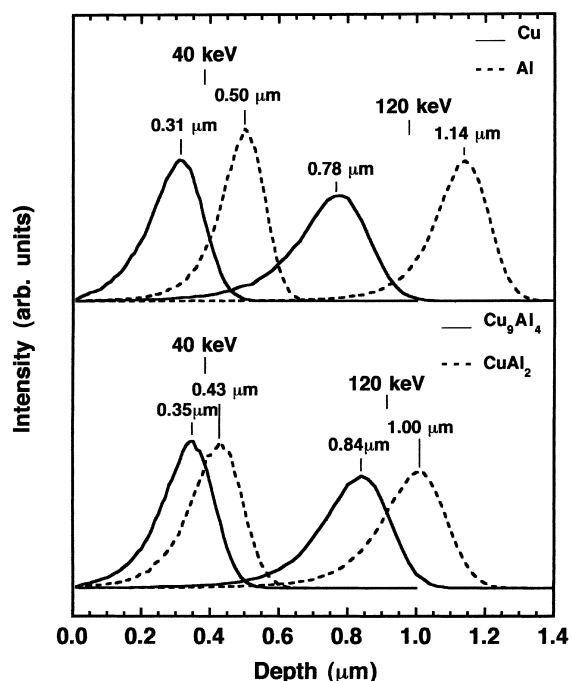


Fig. 1. Implantation depth profiles of deuterium in Cu, Al, Cu₉Al₄ and CuAl₂ as calculated by the TRIM program. Ions are incident normal to the surfaces.

3.3. SIMS profiles of Cu, Al and O

SIMS sputter depth profiles (negative secondary ion signals versus sputtering time) of Cu, Al and O in coatings of different weights implanted with deuterium under identical conditions (samples 8–10 in Table 1) are presented in Fig. 2(a)–(c). The Cu and the Al signals are enhanced to make them viewable on the linear scale (multiplication factors are given in the figure). The depth axis in this figure and the following figures is based on an average sputtering rate obtained by the profilometer measurements of the depths of the craters left behind at the end of sputtering. In each coating, the Cu signal is high and constant, and decreases rapidly as the interface is reached. All coatings yield low Al signals at the surface and these signals increase with increasing depth below the surface indicating Al gradients in the coatings. The Al signals originate from the substrate where the Cu signals begin to decrease rapidly. The source of Al in the coatings is most likely the Al that sputtered off of the Al-6061 substrates during the initial Ar⁺ plasma cleaning stage and condensed on the steel substrate holder. During subsequent Cu deposition, this Al re-sputtered and re-condensed on the growing Cu layer. The gradual

decrease in the Al signal from the interface to the surface suggests that the supply of Al is exhausted with increasing deposition time. As far as the O signals are concerned, after peaking at the surface (surface adsorbed oxygen and/or surface oxide), the O counts decrease rapidly before rising again to a maximum. The counts then decrease continuously with increasing depth. The O signals peak just where the Al signals reach the saturation value and the Cu signals begin to decrease rapidly. These positions mark the original substrate surface and match well with the calculated coating thicknesses (based on density and geometry considerations). Obviously, oxygen is present at the coating–substrate interface and the interface oxygen content decreases with increasing coating weight (thickness) as evidenced by decreasing SIMS signal with increasing coating weight. The observation suggests that the deposition process begins with a substantial amount of oxygen in the plasma and, therefore, in the coating. As the sputter deposition proceeds, the plasma becomes cleaner (devoid of oxygen) and so does the coating. The plasma becomes cleaner with time because the oxygen adsorbed on the vacuum vessel walls (and other surfaces) is knocked off by the plasma and is subsequently removed by the pumping system. Significant presence of Cu and Al on either side of the original surface indicates substantial interdiffusion between Cu and Al. Similar behavior was observed in other coatings.

3.4. Comparison of deuterium implantation in Al and in Cu coated Al

Two Al-6061 samples without any copper coating were implanted with deuterium under monoenergetic (40 keV) and multienergetic (40 + 120 keV) implant conditions at a fluence of 1×10^{21} D⁺/m² (samples 1 and 2 in Table 1). SIMS sputter depth profiles of deuterium in the two samples are shown in Fig. 3(a). At any given sputtering time, the deuterium counts are higher in the sample implanted under multienergetic conditions as compared to monoenergetic implantation. Once implanted, deuterium diffuses towards the front surface (surface exposed to the deuterium flux) and the back surface as a result of the concentration gradients (high in the implantation region, decreasing towards both surfaces). During its migration towards the front surface, deuterium can be trapped by vacancies and vacancy clusters which are produced in the target as a result of deuterium implantation (implantation of deuterons in Al-6061 at 40 and 120 keV will produce displacement cascades in the samples [15,21]) and by the oxide layer near the surface. This continuous trapping of deuterium by the implantation induced defect sites and by the oxide layer near the surface probably suppresses the expected bell shaped implantation profile. Due to the larger concentration of defects induced in the

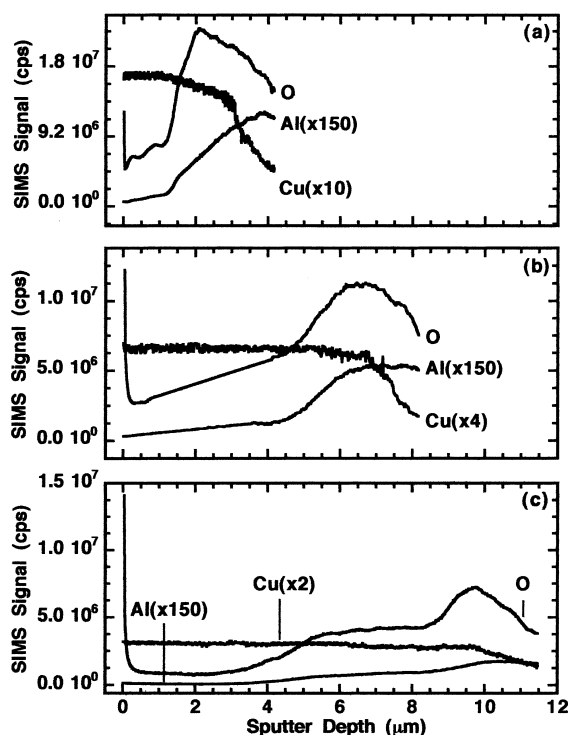


Fig. 2. SIMS sputter depth profiles of Cu, Al and O as a function of coating weight under identical implantation conditions: (a) sample 8, (b) sample 9 and (c) sample 10. For coating weights and implantation conditions, refer to Table 1.

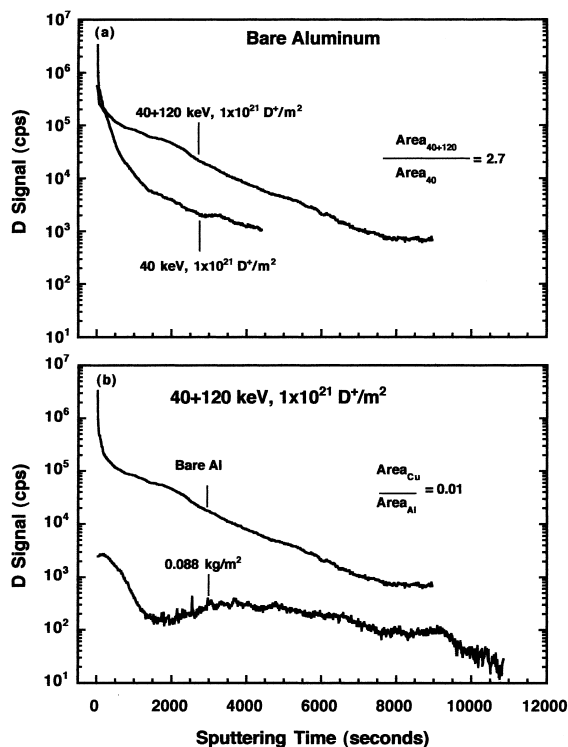


Fig. 3. SIMS sputter depth profiles of deuterium implanted in: (a) bare Al-6061 samples 1 and 2 and (b) bare Al sample 2 and sample 10 which is 0.088 kg/m² coating. For implantation conditions refer to Table 1.

multienergetically implanted sample as a result of higher implantation energy, the deuterium retention, which is proportional to the area under each curve, should be higher in that sample. This is indeed the case because up to 4405 s, which is the total sputtering time for sample 1, the ratio of the areas under the two curves, A_{40+120}/A_{40} , is equal to 2.7.

Comparison of deuterium depth profiles in bare Al-6061 and Al-6061 coated with Cu (0.088 kg/m²) is presented in Fig. 3(b). It is obvious that deuterium retention in the Cu coated sample is smaller than in the bare Al-6061 sample (up to any given sputtering time, the area under the Cu coated sample is smaller than the area under the bare Al-6061 sample). For example, up to 8960 s (which is the maximum sputtering time for the bare Al-6061 substrate, sample 2), the ratio of the area under the Cu coated sample to the area under the bare Al-6061 sample is 0.01. It can be argued that the above comparison is not reasonable because under identical sputtering conditions Al sputters at a slower rate than Cu. Therefore, for the same sputtering time, Cu will be sputtered to a higher depth than Al. A more meaningful comparison would be based on sputtering depth rather than sputtering time. Unfortunately, the sputtering rate

of bare Al-6061 sample was not measured in this study. However, if in Fig. 3(b), D signals could be plotted versus sputter depth rather than time, the data would indicate an even higher relative retention of deuterium in the bare Al-6061 sample. To provide the reader some feel for the magnitude of this effect, TRIM simulation code was used to calculate the sputtering yields of Al and Cu due to bombardment of the surfaces (at room temperature) by 14.5 keV Cs⁺ at an incidence angle of 24.5° with respect to surface normal (actual incidence angle). The calculations reveal the sputtering yield of Cu to be 60% higher than that of Al. Another aspect that makes this direct comparison difficult is the phenomenon known as matrix effect [22]. Matrix effects lead to slight peaking of D signal in regions where O signal is high. Since Al has higher affinity for oxygen as compared to Cu, it is logical to assume that matrix effects will be more pronounced in the bare Al-6061 sample as compared to the Cu coated sample, perhaps resulting in an artificially higher D count in the Al-6061 compared to Cu. However, in this study negative SIMS was carried out, for which the matrix effects are somewhat less pronounced [23].

Higher retention of deuterium in bare Al-6061 as compared to the Cu coated sample can be attributed to the following reasons: (i) Al is a stronger oxide former than Cu and has a natural oxide layer on its surface which leads to deuterium entrapment, and (ii) the maximum energy transferred to Cu atoms from the incident deuterium ions is smaller (5 and 15 keV for implantation at 40 and 120 keV, respectively) than the energy transferred to Al atoms from the incident deuterium ions (10 and 30 keV for implantation at 40 and 120 keV, respectively), which leads to lower defect concentrations in Cu. The lower irradiation induced defect concentration and lower surface oxygen content in Cu as compared to Al will lead to higher transport rate and higher recombination rate of deuterium in Cu, resulting in lower deuterium retention.

3.5. Effect of coating thickness on deuterium profile

SIMS sputter depth profiles of deuterium implanted in copper coatings of different weights under identical conditions (samples 8–10 in Table 1) are shown in Fig. 4. In all three coatings, deuterium signals start from a relatively low value, peak at ~0.2 μm below the surface and then decrease till background signal level is reached. In the 0.03 kg/m² coating another peak centered at ~0.43 μm is clearly visible, while in the 0.06 and the 0.088 kg/m² coatings, broad peaks centered at ~1.5 and ~4 μm, respectively are also visible. The deuterium depth profiles do not show the peaks corresponding to deuterium implantation in Cu at 40 and 120 keV. These peaks should be centered around 0.31 and 0.78 μm, respectively. The existence of sharp deuterium peaks at

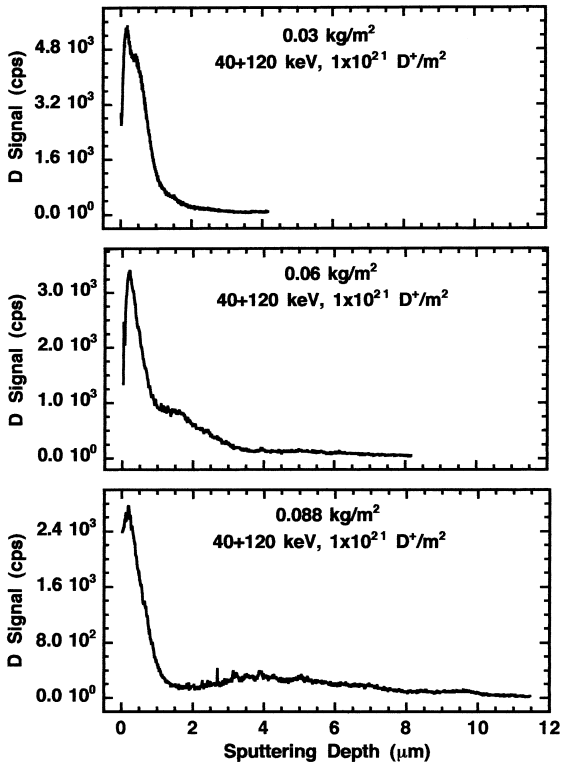


Fig. 4. SIMS sputter depth profiles of deuterium implanted in coatings of different weights under identical conditions.

depths smaller than the ion range, and broad deuterium peaks at depths much greater than the ion range indicates deuterium migration in both directions and re-trapping. Perhaps there is ion induced removal of deuterium from the traps in the implant zone with re-trapping near the surface and beyond the ion range. To assess the nature of these traps, oxygen sputter depth profiles in the same samples were considered. These are shown in Fig. 2(a)–(c). Deuterium profiles do not appear to correlate with the corresponding oxygen profiles. However, a minor case may be made for the 0.03 kg/m² coating where the deuterium peak at 0.2 µm correlates well with slight peaking of oxygen at the same location. The permeation of deuterium beyond the ion range may be attributed to other factors as well. First possibility involves room temperature thermal diffusion of implanted deuterium. Although room temperature thermal diffusivities of H₂ in Cu and Al are small, the process may be important given the long time lag between deuterium implantation and SIMS analysis. Another possibility involves local heating effects induced by the Cs⁺ beam during sputter depth profiling. Energetic Cs⁺ ions upon impacting Cu atoms in the coating lose some of their energy which in turn is picked up by the Cu atoms. Due to their high energies, these Cu atoms slow

down over distances larger than the lattice spacing and, therefore, displace many more lattice atoms. Secondary and tertiary recoils that are formed also have enough energy to displace other lattice atoms, and so on, leading to the formation of a collision cascade [21]. The temperature in the collision cascade may rise to several thousands of degrees in the few pico-second time domain, giving sufficient energy to a local region for enhanced diffusion of deuterium.

3.6. Effects of implantation fluence and energy on deuterium profile

SIMS sputter depth profiles of deuterium implanted in the 0.06 kg/m² Cu coatings as a function of deuterium fluence and ion energy (samples 4, 6, 7, 9, 11 and 12 in Table 1) are presented in Fig. 5. Perusal of the figure indicates that as the fluence increases, the deuterium counts at any depth below the surface and subsequently the overall retention increases. One noticeable point is the decrease in the height of the 0.2 µm peak with increasing fluence. Since higher fluence results in generation of more defect sites in the coating (near the surface), entrapment of deuterium at these sites close to the

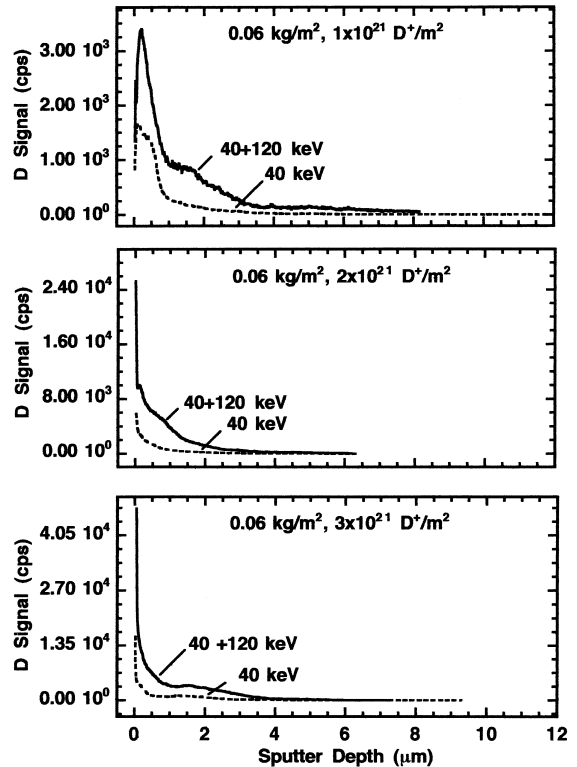


Fig. 5. SIMS sputter depth profiles of deuterium implanted in the 0.06 kg/m² Cu coatings as a function of deuterium fluence and deuterium ion energy.

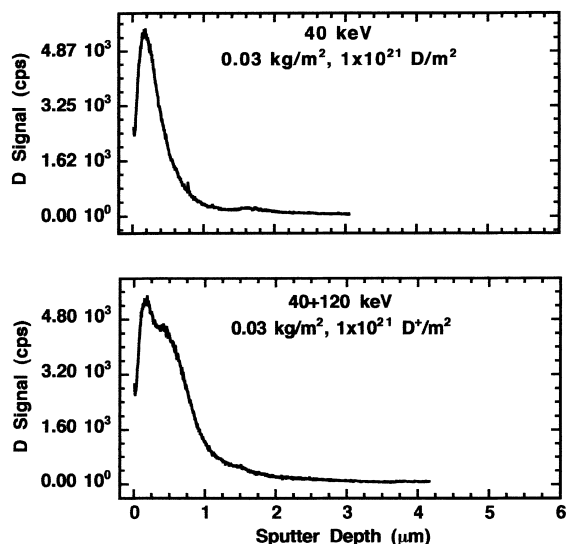


Fig. 6. SIMS sputter depth profiles of deuterium implanted in the 0.03 kg/m^2 Cu coatings as a function of deuterium ion energy.

surface may be one reason for the observed behavior. The other possible reason is the entrapment of deuterium at surface bound oxygen and/or a thin surface oxide layer. Although Cu has a lower tendency to form oxide as compared to Al, surface bound oxygen can still trap deuterium. This can also suppress the expected bell shaped implantation profile. Other deuterium implantation studies in Cu at these and higher implantation fluences also show strong trapping at and near the surface due to radiation induced vacancies and vacancy clusters together with surface oxygen [24].

Fig. 5 also shows the effect of ion energy on SIMS sputter depth profiles of deuterium in the 0.06 kg/m^2 coating at different implantation fluences. Similar data for the 0.03 kg/m^2 coating at a fluence of $1 \times 10^{21} \text{ D}^+/\text{m}^2$ (samples 3 and 8 in Table 1) are presented in Fig. 6. Both figures indicate that the overall deuterium retention in the coatings increases when implantation is carried out at two ion energies instead of one.

3.7. Retention, permeation and release

SIMS analysis provided qualitative data on the retention of deuterium in the coatings. SIMS data was quantified by using NRA [25]. Three 0.06 kg/m^2 coatings implanted at 40 keV & $1 \times 10^{21} \text{ D}^+/\text{m}^2$, 40 keV & $3 \times 10^{21} \text{ D}^+/\text{m}^2$ and 40 + 120 keV & $3 \times 10^{21} \text{ D}^+/\text{m}^2$ (samples 4, 7 and 12 in Table 1) were analyzed by NRA. The deuterium depth profile obtained by NRA in sample 7 is shown in Fig. 7. Due to the limited statistics and

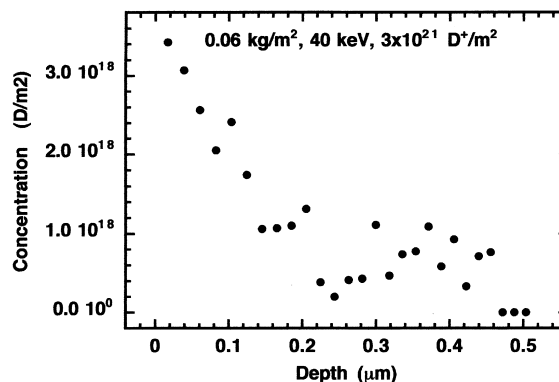


Fig. 7. Deuterium depth profiles in the 0.06 kg/m^2 coatings using ^3He nuclear reaction. Implantation conditions are shown in the figure.

resolution of the profiling technique, the data are plotted up to a depth of $0.5 \mu\text{m}$. Similar data were obtained for the other two samples. The total amount of deuterium retained in each sample up to $0.5 \mu\text{m}$ (as determined by NRA) are plotted versus the areas under the corresponding SIMS sputter depth profiles up to the depth of $0.5 \mu\text{m}$ in Fig. 8. A linear relationship exists between the amount of deuterium retained and the area under the SIMS sputter depth profile (the line equation is shown in the figure). This linear plot was used to calculate the retention of deuterium in various samples from the knowledge of the areas under the SIMS profiles (up to $4 \mu\text{m}$). This calculation is based on the assumption that the linear relationship holds even at higher areas (implantation depths). The retention of deuterium is presented in Fig. 9(a)–(b) as a function of the two variables. The figure indicates that the deuterium retention: (a) decreases initially with increasing coating weight and then levels off with further increase in coating weight, and (b) increases linearly with deuterium implantation

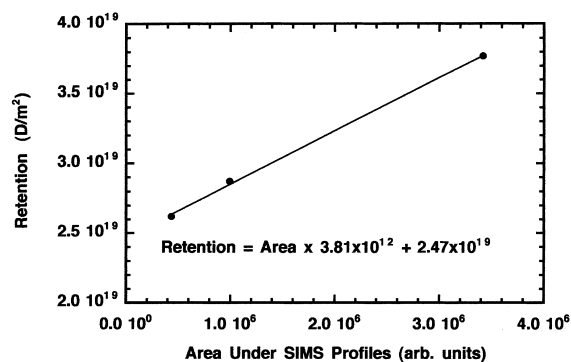


Fig. 8. Relationship between deuterium retention measured by NRA and area under the SIMS sputter depth profile.

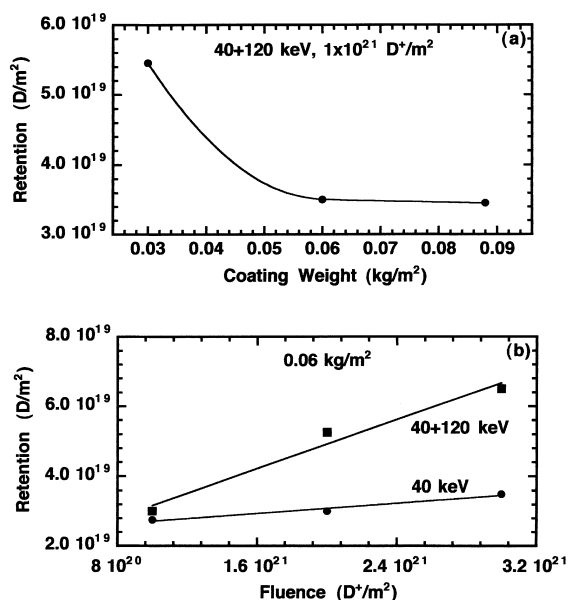


Fig. 9. Deuterium retention as a function of: (a) coating weight and (b) fluence.

fluence under both mono and multi-energetic implant conditions.

To interpret the decrease in deuterium retention with increasing coating weight, an attempt was made to correlate deuterium retention in the coatings with the oxygen level in the coatings. For this purpose the oxygen levels in the coatings of different weights were examined. Since deuterium retentions in the coatings were measured up to 4 μm depth, oxygen levels in the corresponding coatings were estimated by determining the areas under the SIMS profiles up to 4 μm depth. These areas decrease in the ratio 1.00:0.25:0.07 as the coating weights increase from 0.03 to 0.06 to 0.088 kg/m². There is a definite correlation between the amount of deuterium retained and the oxygen level in the coatings. It is possible that decreasing deuterium retention with increasing coating weight is due to decreasing oxygen content of the coatings with increasing coating weights.

Higher deuterium retention with increasing fluence (Fig. 9(b)) has been observed in other studies, as well. In Cu coated Al-6061 samples, the linear behavior is seen up to a fluence of 1×10^{22} D⁺/m². Beyond this fluence, the curve levels off [26]. Multiple energy implantation also leads to higher retention. The effect of fluence can be explained by the fact that since increasing fluence results in the generation of more irradiation induced defect sites in the implantation region, more deuterium is trapped at these sites during its migration to the coating surface, leading to higher retention.

4. Conclusions

The potential of Cu coatings deposited on Al-6061 substrates was evaluated for minimizing the retention and permeation of implanted deuterium. Deuterium retention in an Al-6061 sample coated with 0.088 kg/m² of Cu was determined to be much smaller as compared to retention in a bare Al-6061 sample indicating that the deuterium release characteristics of Cu are better than that of Al-6061. At higher deuterium fluences, a high concentration of deuterium was observed near the surface probably due to trapping of migrating deuterium atoms at the implantation induced defect sites (vacancies and vacancy clusters). SIMS and NRA data indicated that deuterium retention initially decreased with increasing coating weight and then leveled off with further increases in coating weight. Moreover, increasing implantation fluence resulted in higher retention in the coatings, with a linear build up behavior. Also the usage of multi-energetic implantation versus mono-energetic implantation led to higher deuterium retention. Under the coating weights and implantation conditions studied, the amount of deuterium retained in the coatings ranged between 1.2% and 5.4% of the implanted amount. The ³He containing Al-6061 tubes in the target/blanket assembly of the accelerator production of tritium reactor, therefore can benefit from an application of Cu coating on the inside surface.

Acknowledgements

This work was supported by the APT Program Office, Los Alamos National Laboratory, under the US DOE Grant DEFG0497AL 77993. SIMS studies were carried out in the Center for Microanalysis of Materials, University of Illinois, which is supported by the US DOE under grant DEFG0291ER45439. We wish to thank J.S. Baker for her assistance in SIMS measurements. A portion of this work was performed at SNL, Livermore, supported by US DOE under contract number DE-AC04-94AL85000.

References

- [1] J.J. Katz, in: R.E. Kirk, D.F. Othmer (Eds.), *Encyclopedia of Chemical Technology*, 4th Ed., vol. 8, Wiley, New York, 1991, p. 17.
- [2] D.V. Winterfeldt, E. Schweitzer, *Interfaces* 28 (1998) 92.
- [3] M.S. Wechsler, L.K. Mansur, C.L. Snead, W.F. Sommer (Eds.), *Materials for Spallation Neutron Sources*, The Minerals, Metals and Materials Society, Warrendale, 1998.
- [4] S.A. Malloy, W.F. Sommer, R.D. Brown, J.E. Roberts, J. Eddelman, E. Zimmermann, G. Wilcutt, in: M.S. Wechsler, L.K. Mansur, C.L. Snead, W.F. Sommer

- (Eds.), *Materials for Spallation Neutron Sources*, The Minerals and Materials Society, Warrendale, 1998, p. 131.
- [5] M.Y. Inal, M. Alam, *Met. and Mater. Trans. A* 30 (1999) 2191.
- [6] P.M. Richards, *J. Nucl. Mater.* 152 (1988) 246.
- [7] S.T. Picraux, *Nucl. Instrum. and Meth.* 182–183 (1981) 413.
- [8] T. Schober, *Phys. Rev. B* 31 (1985) 7109.
- [9] S.M. Myers, F. Besenbacher, J. Norskov, *J. Appl. Phys.* 58 (1985) 1841.
- [10] S.M. Myers, D. Follstaedt, *J. Nucl. Mater.* 145–147 (1987) 322.
- [11] K. Kamada, A. Sagara, N. Sugiyama, Y. Yamaguchi, *J. Nucl. Mater.* 128&129 (1984) 664.
- [12] T. Hayashi, K. Okuno, K. Yamanaka, Y. Naruse, *J. Alloys Comp.* 189 (1992) 195.
- [13] S. Yamaguchi, S. Nagata, K. Takahiro, S. Yamamoto, *J. Nucl. Mater.* 220–222 (1995) 878.
- [14] T. Tanabe, Y. Furiyama, N. Saitoh, S. Imoto, *Trans. Jap. Inst. Met.* 28 (1987) 706.
- [15] W. Möller, J. Roth, in: D.E. Post, R. Behrisch (Eds.), *Physics of Plasma Wall Interactions in Controlled Fusion*, NATO Advanced Science Institute Series, Series B: Physics vol. 131, Plenum, New York, 1986, p. 439.
- [16] C.L. Mantel, *Engineering Materials Handbook*, McGraw Hill, New York, 1958, p. 36.41.
- [17] M.Y. Inal, M. Alam, R.A. Peascoe, T.R. Watkins, Residual stress determination in deuterium implanted copper coatings deposited on Al-6061 substrates, *J. Mater. Res.*, in press.
- [18] J.F. Ziegler, J.P. Biersack, U. Littmark, *The Stopping and Range of Ions in Solids*, Pergamon, New York, 1985.
- [19] A.H. Wapstra, N.B. Gove, *Atomic Mass Table – Part 1*, *Nuclear Data A*, vol. 9, 1971, p. 267.
- [20] JADE 3.3 – PDF Card Numbers 04-0787, 04-0836, 24-0003 and 25-0012, *Materials Data Inc.*, Livermore, 1997.
- [21] H. Ullmaier, *MRS Bull.* 22 (1997) 14.
- [22] R.G. Wilson, F.A. Stevie, C.W. Magee, *Secondary Ion Mass Spectrometry*, Wiley, New York, 1989, p. 2.3-1.
- [23] R. Bastasz, Sandia National Laboratory, Livermore, CA, private communications.
- [24] B. Panigrahi, K.G.M. Nair, K. Krishan, *Bull. Mater. Sci.* 19 (1996) 61.
- [25] J. Böttiger, *J. Nucl. Mater.* 78 (1978) 161.
- [26] D.F. Cowgill, R.A. Causey, Tritium retention and permeation through aluminium APT tubes, *J. Nucl. Mater.*, to be published.